FOURTH EUROPEAN ROTORCRAFT AND POWERED LIFT AIRCRAFT FORUM

Paper No. 17

THE ROLE OF ROTOR IMPEDANCE IN THE VIBRATION ANALYSIS
OF ROTORCRAFT

K. H. Hohenemser
Washington University, St. Louis, Missouri

S. K. Yin
Bell Helicopter Textron, Fort Worth, Texas

USA

September 13 - 15, 1978

Stresa - Italy

The Role of Rotor Impedance in the

Vibration Analysis of Rotorcraft

Kurt H. Hohenemser

Washington University, St. Louis, Missouri

Sheng-Kuang Yin

Bell Helicopter Textron, Fort Worth, Texas

Abstract

As an alternative to a total system vibration analysis with its
lack of visibility of critical dynamic parameters, one often first
determines the dynamic rotor forces and moments acting on a rigid
support, and one then excites the flexible airframe-less-rotor with
these inputs. In an improved method which still retains the advantage
of separate treatment of rotor and airframe, the rotor impedance is
used to correct the input to the airframe. This improved method is
illustrated for a strongly idealized case of vertical excitation and
then for rolling and pitching moment excitation of a four bladed
hingeless rotor on an up-focussing flexible mount. Contrary to the
usual approach that represents aeroelastic blade motions by a series
of normal blade modes in vacuum, the aeroelastic rotor impedances are
computed directly with a finite blade element method that includes
aerodynamics. The rotor impedance matrix for 3 or more blades is
determined from the root moment impedance for a single blade by a
simple multiblade transformation rule. Force and moment amplitudes
transferred from the rotor to the support are found to be critically
dependent on the support dynamics. Thus the rotor impedance is shown
to be an essential item in the vibration analysis.

$\overline{EI}$	EI/EI_0, flap-bending stiffness over root value
$[E]$	transfer matrix across massless blade element
$[F]$	transfer matrix across point mass
I_b/I	blade moment over support moment of inertia
M	blade flap-bending moment, unit $\rho_0 R^3 \Omega^2$
M/M_0	rotor moment on flexible over moment on rigid support
N	number of finite elements per blade
P,Q	polynomials of λ
Q_R, Q_S	rotor and support impedances
R	rotor radius
S	blade shear force, unit $\rho_0 R^2 \Omega^2$
T	blade tension force, unit $\rho_0 R^2 \Omega^2$
X	state vector
a	blade airfoil lift slope
b	number of blades in rotor
c	blade chord, unit R
c_i	aerodynamic damping coefficient at ith station
f/f_0	rotor force on flexible over force on rigid support
g_i	aerodynamic coefficient for blade pitch angle
l_i	length of blade element, unit R
m_R	one half rotor vertical mass
m_S	support mass
m_i	point mass at station i, unit $\rho_0 R$
p	$(T/q\,\overline{EI}\,)^{1/2}$ blade tension force parameter
q	$EI_0/\rho_0 R^4 \Omega^2$ blade root flap-bending stiffness
$q^{-1/2}$	speed parameter
r_i	distance of blade station i from rotor center, unit R
t	time, unit $1/\Omega$
y	blade deflection, positive up, unit R
z	a single blade variable
Θ	blade pitch angle, positive up
$[\phi]$	$[E]\,[F]$, transfer matrix
ψ_k	azimuth angle of kth blade

Ω	rotor angular speed
α	hub tilt angle
γ	$3\rho ac$, Lock number for uniform blade
ζ	real part of complex valued frequency, unit Ω
λ	$\zeta \pm i\omega$, complex valued frequency, unit Ω
ρ	air density, unit ρ_0/R^2
ρ_0	blade mass per unit length at blade root
ω	excitation circular frequency, unit Ω
ω_N	coupled natural frequency, unit Ω
ω_R	rotor uncoupled natural frequency, unit Ω
ω_S	support uncoupled natural frequency, unit Ω (also ω_I, ω_{II})
ω_{SN}	support uncoupled natural frequency producing $\omega_N = \omega$
$\bar{\omega}_R, \bar{\omega}_S$	ω_R/ω, ω_S/ω, frequency ratios

Subscripts

I, II	multiblade coordinates, forward and left respectively
i	outer end of blade element, beginning with 1 at blade tip
12, 13	elements of a matrix or determinant
I, R	imaginary, real parts of a polynomial
M, α, Θ	polynomials multiplied by M_{N+1}, α, Θ

Superscripts

$\cdot$	time differentiation
$'$	length differentiation

Introduction

Recently, a great deal of attention has been paid to the problem of rotorcraft vibrations. It is generally accepted that rotorcraft vibrations should be alleviated because they reduce crew proficiency, cause passenger discomfort, produce equipment deterioration and structural fatigue, and increase maintenance. Fig. 1 taken from reference 1 shows the cockpit vibration exposure limits at cruise speed in terms of hours of maintained crew proficiency vs. frequency in Hz according to guidelines in reference 2. The indicated cruise vibration level for UTTAS and AAH shows substantial improvement over their predecessors, the UH-1 and the AH-1. Part of the improvement is caused by the increase in vibration frequency when going from a 2 bladed to a 4 bladed rotor, since humans are less affected by vibratory accelerations at frequencies above 10 Hz.

Presently vibration prediction methods are not reliable. There is hardly a rotorcraft prototype which did not exhibit during initial flight testing excessive vibrations. Their reduction to specification level usually requires an intensive, costly, time and payload consuming effort. The vibration level is often sensitive to small variations in dynamic parameters so that two rotorcraft from the same production run can have substantial differences in vibration level. There are a variety of vibration sources. Most important is usually main rotor excitation with the blade passage frequency which will be the topic of this paper. Other sources of vibrations are higher rotor harmonics particularly with twice blade passage frequency, rotor wake excitation of the empenage, mass, aero, and damper unbalances, rotor self-excitation leading to limit cycles, and parametric rotor excitation leading to fractional harmonics. Each of these vibration sources requires different measures of alleviation. For main rotor excitation of the airframe the most important means of vibration control is the proper selection of the frequency spectrum for rotor and airframe. Other means are passive blade pitch control, active higher harmonic blade pitch control (not as yet flight tested), rotating system absorbers (pendulum, bifilar), fixed system absorbers, preferably self-tuning,

and the various means of passive and active rotor isolation. The
vibration prediction method to be discussed here is applicable to all
of these dynamic configurations, since they all require a fully coupled
rotor/airframe analysis.

Rotor/Airframe Impedance Matching

Coupled rotor/airframe vibrations can be and have been treated by
total system analysis, see for example references 3 to 5. The large
computer programs needed for such an analysis can easily obscure the
influence of crucial dynamic parameters on the vibration level. More
visibility for such parameters is achieved by performing separate
vibration analyses (or testing) for the rotor and for the airframe and
by then matching dynamic forces, moments and deflections at the inter-
face. In its crudest form of matching the rotor reactions on a rigid
support are first determined and then applied to the flexible airframe
to establish its response. The design goal is to avoid airframe
resonances to the dynamic rotor inputs. Fig. 2 shows the results of
such an airframe response analysis taken from reference 4. The graph
gives the vertical acceleration amplitude at the pilot station from
$\pm$ 10,000 inch pounds pitching moment input at the rotor hub vs. the
excitation frequency for various ballast distributions of the AH-56A(AMCS)
helicopter. While the trend is probably true, the results do not
include the effects of the ballast changes on the rotor moment input.
These effects may be substantial.

A better approximation is obtained when an equivalent hub mass is
added that is representative of the rotor impedance at the excitation
frequency. As outlined for example in reference 5, this method of
establishing the airframe response to rotor dynamic inputs has its
limitations. The equivalent masses are different for horizontal and
vertical motions, and the equivalent mass concept also does not consider
aerodynamic damping effects. The correct way of dynamically matching
rotor and airframe is to determine the impedance or mobility matrices
of both substructures at the interface and to write the compatibility

relations for the interface forces and deflections. Reference 5
presents a simple example for this method. Since the cruder method of
exciting the airframe with separately determined rotor input forces is
suggested in textbooks (references 6 and 7) and is also practiced in
industry, it was believed worthwhile to apply the method of impedance
matching to a more complex example and to demonstrate the large changes
in rotor input to the airframe caused by dynamic rotor/airframe
coupling.

The principle of rotor/airframe impedance matching is seen in
Fig. 3. A rotor on a rigid support is schematically shown in Fig. 3a.
The force amplitude on the support is f_0. This symbol should be
interpreted as the column of complex valued force and moment ampli-
tudes that the rotor transmits to the rigid support. Fig. 3b shows a
rotor supported by an airframe. Here f represents the dynamic force
column, z the deflection column including angular deflections. The
force f is equal to f_0 minus the rotor reaction force due to the
deflection z at the rotor/airframe interface.

$$f = f_0 - Q_R(\lambda) \ z \qquad (1)$$

where $Q_R(\lambda)$ is the rotor impedance. The same force f acts on the
airframe or rotor support and produces the same deflection z

$$f = Q_S(\lambda) \ z \qquad (2)$$

where $Q_S(\lambda)$ is the airframe or support impedance. By inserting Eq. (2)
into Eq. (1) one obtains

$$f = (I + Q_R(\lambda) \ Q_S(\lambda)^{-1})^{-1} \ f_0 \qquad (3)$$

I is the identity matrix.

Rotor and Support Representation by 3 Masses and 2 Springs

Before deriving the impedance matrix for an actual rotor, a quantitative interpretation of Eq. (3) will be given for the simple system defined in Fig. 4. The rotor is represented by two vertically moving equal masses m_R interconnected by a spring with stiffness K_R. The rotor support is represented by a mass m_S and by a spring with stiffness K_S. A dynamic force f_o with imaginary frequency λ acts on the support mass m_S if this mass is rigidly held. The impedances are now polynomials of λ and Eq. (3) can be written

$$f/f_0 = (1 + Q_R(\lambda) \; Q_S(\lambda)^{-1})^{-1} \qquad (4)$$

Introducing

$$\omega_R^2 = K_R/m_R \quad , \quad \omega_S^2 = K_S/m_S \qquad (5)$$

it is easy to show that

$$Q_R(\lambda) = m_R(\lambda^2 + \omega_R^2/(1 + (\omega_R/\lambda)^2)) \qquad (6)$$

$$Q_S(\lambda) = m_S(\lambda^2 + \omega_S^2) \qquad (7)$$

Inserting Eqs. (6) and (7) into Eq. (4)

$$f/f_0 = [1 + (m_R/m_S)(\lambda^2 + \omega_R^2/(1 + (\omega_R/\lambda)^2)/(\lambda^2 + \omega_S^2)]^{-1} \qquad (8)$$

Selecting a time scale such that $\omega_R = 1$ we have for $f/f_o = \infty$ the characteristic equation

$$\lambda^4(1 + m_R/m_S) + \lambda^2 (\omega_S^2 + 1 + 2 \; m_R/m_S) + \omega_S^2 = 0 \qquad (9)$$

Since the system is conservative the roots of Eq. (9) are purely imaginary, $\lambda = i\omega$. For $\omega_R = K_R = 0$ one has the natural frequency

$$\omega_N = \omega_S / (1 + m_R/m_S)^{1/2} \qquad (10)$$

For $\omega_R = K_R = \infty$ the natural frequency is

$$\omega_N = \omega_S / (1 + 2 \, m_R/m_S)^{1/2} \qquad (11)$$

Eqs. (10) and (11) follow from Eq. (8) for $f/f_0 = \infty$. They are also directly evident from Fig. 4. In the first case the spring K_S carries the mass $m_R + m_S$ and is uncoupled from the upper mass m_R. In the second case the spring K_S carries the mass $2 \, m_R + m_S$.

For $\omega_R = 1$ and $m_R/m_S = 2.5$ the roots of Eq. (9) are only dependent on the support uncoupled frequency ω_S. They are shown vs. ω_S in Fig. 5. The higher of the two natural frequencies is for large ω_S asymptotic to the value of Eq. (10) for $\omega_R = 0$. The lower natural frequency is asymptotic to the line $_R = 1$. This asymptotic behavior for large ω_S or K_S is also directly evident from Fig. 4. Inserting $\lambda = i\omega$ into Eq. (8) and introducing $\overline{\omega}_R = \omega_R/\omega$, $\overline{\omega}_S = \omega_S/\omega$ one obtains

$$f/f_0 = [1 - (m_R/m_S)(1 + \overline{\omega}_R^{-2}/(\overline{\omega}_R^{-2} - 1))/(\overline{\omega}_S^{-2} - 1))]^{-1} \qquad (12)$$

Vertical Force Excitation

For a numerical example we select the case of Fig. 5 with $\overline{\omega}_R = 1$, $m_R/m_S = 2.5$ and stipulate that the forcing function frequency be $\omega = 1.89$. Now $\overline{\omega}_R = 1/1.89 = .53$ and Eq. (12) becomes

$$f/f_0 = (1 - 1.53/(\overline{\omega}_S^{-2} - 1))^{-1} \qquad (13)$$

For $\overline{\omega}_S = 1$ when the excitation frequency ω is equal to the uncoupled support frequency ω_S, the ratio f/f_0 is zero. Absolute values from Eq. (13) are plotted in Fig. 6. It is seen that the input to the support mass m_S depends critically on the support stiffness as expressed by the ratio $\overline{\omega}_S = \omega_S/\omega$.

Eq. (13) can also be derived in a different way making use of the value ω_{SN} associated with the coincidence of excitation frequency ω with the coupled system natural frequency ω_N. At this frequency $f/f_0 = \infty$ or $f_0 = 0$ and we have from Eq. (4)

$$Q_R(\omega_N) = - Q_S(\omega_N) \tag{14}$$

Thus Eq. (4) becomes

$$f/f_0 = (1 - Q_S(\omega_N) \, Q_S(\omega)^{-1})^{-1} \tag{15}$$

Inserting the support impedances from Eq. (7)

$$f/f_0 = (1 - (\omega_{SN}^2 - \omega_N^2)/(\omega_S^2 - \omega^2))^{-1} \tag{16}$$

Stipulating $\omega_N = \omega$ and using as before $\bar{\omega}_S = \omega_S/\omega$

$$f/f_0 = (1 - (\bar{\omega}_{SN}^2 - 1)/(\bar{\omega}_S^2 - 1))^{-1} \tag{17}$$

For the example of Fig. 6 we have $\bar{\omega}_{SN} = 3/1.89 = 1.59$ and Eq. (17) reduces to Eq. (13). Eqs. (15) and (17) are particularly convenient since they use only support data and no rotor data, except that the support stiffness resulting in a coupled natural frequency of $\omega_N = \omega$ must be known. Eq. (17) will be used later in connection with a more complete rotor analytical model.

It is also of interest to determine the springforce amplitude f_s that the support spring transmits to the base, see Fig. 4. One can easily derive the expression

$$f_s/f_0 = \bar{\omega}_S^{-2}/(\bar{\omega}_S^{-2} - \bar{\omega}_{SN}^{-2}) \tag{18}$$

The absolute values are plotted in Fig. 7 vs. $\bar{\omega}_S$ assuming as before $\bar{\omega}_{SN} = 1.59$. The spring force amplitude is smaller than the rotor excitation force f_0 when $\bar{\omega}_S < 1.1$. Fig. 7 also shows the base input

f_s/f_o for $f/f_o = 1.0$ according to

$$f_s/f_o = \overline{\omega}_S^2/(1 - \overline{\omega}_S^2) \qquad (19)$$

For low support stiffness this base input is much larger than the actual value, indicating again the error encountered when ignoring rotor-support coupling.

For a DAVI type of support (Dynamic Antiresonance Vibration Isolator, see for example references 8 and 9) with a large ratio of $1/a$, see Fig. 8, and with an equivalent absorber mass $m_A = m (1/a)^2$ the force amplitude transferred to the base is

$$f_s/f_o = (\overline{\omega}_S^2 - m_A/(m_s + m_A))/(\overline{\omega}_S^2 - \overline{\omega}_{SN}^2) \qquad (20)$$

This base force is zero for

$$\omega_S = (m_A/(m_A + m_S))^{1/2} \qquad (21)$$

The ratio f_s/f_o for $m_A/m_S = 1$ and for the same $\overline{\omega}_{SN} = 1.59$ as before is also shown in Fig. 7. Zero base input occurs at $\omega_S = .7$. At this low support stiffness the base input without DAVI is already rather low, namely $f_s/f_o = .3$.

From the preceding example it is evident that the excitation of the airframe with the rotor force acting on a rigid support can lead to large errors in the response. When the excitation frequency coincides with an uncoupled natural airframe frequency, one would erroneously obtain a large resonance response, while actually the response is modest and no force is transmitted to the airframe.

Rolling and Pitching Impedance Analysis for a Hingeless Rotor

The following rotor impedance analysis neglects chordwise blade vibrations and is limited to zero advance ratio. The rotor impedance is not expected to vary drastically with advance ratio as long as the

advance ratio is moderate. Thus the use of rotor inputs to a rigid
support at a given advance ratio together with the impedance at zero
advance ratio should result in a reasonable approximation for the
vibration prediction. Within the advance ratio range in which a
constant coefficient multiblade rotor representation is feasible
(reference 10) it is easy to apply corrections from non-zero advance
ratio. Only when periodic coefficients are required also in multi-
blade coordinates will it be necessary to reformulate the rotor imped-
ance problem.

The impedance analysis uses blade element transfer matrices
similar to those described in reference 11. Each blade element has
constant bending stiffness and is free of distributed loads. The
stiffness can vary stepwise from element to element. Point loads are
assumed to act at the element boundaries. Except for the stepwise
stiffness variation and .except for the point loads at the element
boundaries the analysis is exact with no further approximations. This
has the advantage that large beam curvature can be admitted for example
in the cantilever blade root section without the need of a large
number of short elements as they are required for the C 81 computer
program. In reference 11 aerodynamic loads are omitted, so that only
vacuum modes and natural frequencies are obtained. They are not
suitable for computing blade or rotor impedances. In reference 11 the
purely imaginary eigenvalues of the blade characteristic equation are
found by trial and error, a method not feasible for non-conservative
systems with complex valued natural frequencies.

The four steps to extend reference 11 method to our problem are
the following:
1. Aerodynamic terms are included in the blade transfer matrix as
   point loads at the element boundaries using quasi steady theory.
2. Relations between blade root state variables are derived in-
   cluding a dynamic blade pitch term.
3. Single blade polynomials are transformed into multiblade matrices
   applicable to 3 or more blades per rotor.
4. Total system equations are derived by mobility or impedance
   matching at the rotor/airframe interface.

Blade Element Transfer Matrix

The computation procedure will be outlined here. More details are given in reference 12. As indicated in the Nomenclature all quantities are non-dimensionalized by using the length unit R, the time unit $1/\Omega$ and the mass unit $\rho_o R$, where ρ_o is the blade mass per unit length at the blade root. The force unit then is $\rho_o R^2 \Omega^2$, the moment unit is $\rho_o R^3 \Omega^2$, etc. A blade element with its inputs at the boundaries is shown in Fig. 9. There are 5 state variables; shear force S, bending moment M, slope y', deflection y, and pitch angle Θ, forming the state vector

$$X = \begin{bmatrix} S \\ M \\ y' \\ y \\ \Theta \end{bmatrix} \qquad (22)$$

The transfer matrix from one element to the next is defined by

$$X_{i+1} = [E]\ [F]\ X_i \qquad (23)$$

The matrix [F] gives the change in state vector from the right side of the mass m_i to its left side. It expresses the effects of vertical inertia force $(-\lambda^2 m_i)$, of the aerodynamic forces from damping and from dynamic blade pitch angle distributed as point forces at the element boundaries $(-\lambda\ c_i,\ g_i)$, and the centrifugal force element from the mass m_i $(-\ m_i\ r_i)$. The matrix [F] also expresses the continuity relations between the right and left sides of the mass m_i.

$$y'_l = y'_r, \quad y_l = y_r, \quad \Theta_l = \Theta_r \qquad (24)$$

The matrix [F] has the form

$$
[F] = \begin{bmatrix} 1 & 0 & 0 & -(\lambda^2 m_i + \lambda c_i) & g_i \\ 0 & 1 & 0 & - m_i \, r_i & 0 \\ 0 & 0 & 1 & 0 & 0 \\ 0 & 0 & 0 & 1 & 0 \\ 0 & 0 & 0 & 0 & 1 \end{bmatrix} \tag{25}
$$

The matrix $[E]$ gives the change in state vector from the left side of the mass m_i to the right side of the mass $m_i + 1$. It represents the exact solution for the bending of a uniform beam under tension.

$$
[E] = \begin{bmatrix} 1 & 0 & 0 & 0 & 0 \\ 1_i & 1 & 0 & 0 & 0 \\ E_{31} & E_{32} & E_{33} & E_{34} & 0 \\ E_{41} & E_{42} & E_{43} & E_{44} & 0 \\ 0 & 0 & 0 & 0 & 1 \end{bmatrix} \tag{26}
$$

where

$$E_{31} = - E_{42} = - (1/T_i) \, (\cosh(p_i l_i) - 1)$$

$$E_{32} = - (1/T_i) \, p_i \, \sinh(p_i l_i)$$

$$E_{33} = E_{44} = \cosh(p_i l_i)$$

$$E_{34} = p_i \, \sinh(p_i l_i) \tag{27}$$

$$E_{41} = (1/T_i) \, (1/p_i) \, \sinh(p_i l_i)$$

$$E_{43} = - (1/p_i) \, \sinh(p_i l_i)$$

$$p_i = (T_i/q \, \overline{EI_i})^{1/2}$$

In comparing these expressions with those given in reference 11 one must note that λ is defined differently leading to the opposite sign of λ^2 in Eq. (25). Also, the unit of circular frequency in reference 11

is $(EI_0/\rho_0 R^4)^{1/2}$. Here it is the angular rotor speed Ω. Introducing the transfer matrix

$$[E] \; [F] = [\phi] \tag{28}$$

Eq. (23) can be written in the form

$$X_{i+1} = [\phi_i] \; X_i \tag{29}$$

For N point masses one obtains by successive transfer matrix multiplication, beginning at the blade tip, for the blade root quantities the following relations

$$
\begin{bmatrix} S_{N+1} \\ M_{N+1} \\ y'_{N+1} \\ y_{N+1} \end{bmatrix}
=
\begin{bmatrix} \phi_{11} & \phi_{12} & \phi_{13} & \phi_{14} \\ \phi_{21} & \phi_{22} & \phi_{23} & \phi_{24} \\ \phi_{31} & \phi_{32} & \phi_{33} & \phi_{34} \\ \phi_{41} & \phi_{42} & \phi_{43} & \phi_{44} \end{bmatrix}
\begin{bmatrix} S_1 \\ M_1 \\ y'_1 \\ y_1 \end{bmatrix}
+
\begin{bmatrix} \phi_{15} \\ \phi_{25} \\ \phi_{35} \\ \phi_{45} \end{bmatrix} \Theta
\tag{30}
$$

The blade state variables with subscript 1 refer to the blade tip, those with the subscript N+1 refer to the blade root assumed to be at the rotor center. The blade pitch angle Θ is assumed to be constant over the blade radius so that the system of Eq. (30) has only 4 equations rather than the 5 of Eq. (29). All elements of $[\phi]$ are polynomials of λ. Eq. (30) completes step 1 of the impedance analysis. The computations of the aerodynamic coefficients c_i and g_i are straight forward and not presented here. For a uniform blade they are proportional to the Lock number γ which in our non-dimensional units is given by $\gamma = 3 \rho a c$.

Blade Root Moment Impedance

We assume zero vertical motion at the rotor center

$$y_{N+1} = 0 \tag{31}$$

The blade tip bending moment and shearforce is zero

$$M_1 = S_1 = 0 \qquad (32)$$

The two remaining tip variables, y'_1 and y_1 will be expressed in terms of the blade root variables by inserting Eqs. (31) and (32) into Eq. (30).

$$\begin{bmatrix} S_{N+1} \\ M_{N+1} \end{bmatrix} = \begin{bmatrix} \phi_{13} & \phi_{14} \\ \phi_{23} & \phi_{24} \end{bmatrix} \begin{bmatrix} y'_1 \\ y_1 \end{bmatrix} + \begin{bmatrix} \phi_{15} \\ \phi_{25} \end{bmatrix} \Theta \qquad (33)$$

$$\begin{bmatrix} y'_{N+1} \\ 0 \end{bmatrix} = \begin{bmatrix} \phi_{33} & \phi_{34} \\ \phi_{43} & \phi_{44} \end{bmatrix} \begin{bmatrix} y'_1 \\ y_1 \end{bmatrix} + \begin{bmatrix} \phi_{35} \\ \phi_{45} \end{bmatrix} \Theta \qquad (34)$$

Computing $\begin{bmatrix} y'_1 \\ y_1 \end{bmatrix}$ from Eq. (34) and substitution into Eq. (33) one obtains after some manipulations for the second of Eq. (33)

$$M_{N+1} \, P_M(\lambda) = y'_{N+1} \, P_\alpha(\lambda) + \Theta P_\Theta(\lambda) \qquad (35)$$

where

$$P_M(\lambda) = \begin{vmatrix} \phi_{33} & \phi_{34} \\ \phi_{43} & \phi_{44} \end{vmatrix} \quad , \quad P_\alpha(\lambda) = \begin{vmatrix} \phi_{23} & \phi_{34} \\ \phi_{43} & \phi_{44} \end{vmatrix}$$

$$P_\Theta(\lambda) = \begin{vmatrix} \phi_{23} & \phi_{33} & \phi_{43} \\ \phi_{24} & \phi_{24} & \phi_{44} \\ \phi_{25} & \phi_{35} & \phi_{45} \end{vmatrix}$$

If the dynamic blade pitch angle Θ is linearly related to the root slope, Eq. (35) can be used to determine the blade root bending impedance M_{n+1}/y'_{N+1}. For a pitch-flap coupling expressed by $\Theta = k\, y'_{N+1}$, the root bending impedance is

$$M_{N+1}/y'_{N+1} = P_\alpha\,(\lambda)/P_M(\lambda) + k\,P_\Theta\,(\lambda)/P_M(\lambda) \qquad (36)$$

Eq. (36) completes step 2 of the impedance analysis.

Transformation to Multiblade Impedance

The relations between single blade and multiblade coordinates are, when only cyclic terms are retained, see reference 10,

$$
\begin{aligned}
(y'_{N+1})_k &= \alpha_I \cos \psi_k + \alpha_{II} \sin \psi_k \\
\Theta_k &= \Theta_{II} \cos \psi_k - \Theta_I \sin \psi_k \\
(M_{N+1})_k &= M_I \cos \psi_k + M_{II} \sin \psi_k
\end{aligned}
\qquad (37)
$$

α_I, M_I, Θ_I refer respectively to nose down hub tilting angle, nose down rotor moment, and nose down cyclic pitch input. α_{II}, M_{II}, Θ_{II} refer to left hub tilting angle, left rotor moment and left cyclic input. Eqs. 37 are easily inverted, for example

$$\alpha_I = (2/b) \sum_{k=1}^{b} (y'_{N+1})_k \cos \psi_k \qquad (38)$$

Eqs. (37) are valid for 3 or more blades, $b \geq 3$.

By differentiating the relation between a single blade variable z and its multiblade counterpart z_I, z_{II}

$$z = z_I \cos t + z_{II} \sin t \qquad (39)$$

with respect to the time t and by replacing $\dot{z}$, $\ddot{z}$ by λz, $\lambda^2 z$, and $\dot{z}_I$, $\ddot{z}_I$ by λz_I, $\lambda^2 z_I$, etc., one can prove a general rule for transforming

single blade polynomials into multiblade polynomials. According to this rule the single blade expression

$$P(\lambda) \ z \tag{40}$$

with $P(\lambda)$ a polynomial, is transformed into the multiblade expression

$$\begin{bmatrix} P_R(\lambda) & P_I(\lambda) \\ - P_I(\lambda) & P_R(\lambda) \end{bmatrix} \begin{bmatrix} z_I \\ z_{II} \end{bmatrix} \tag{41}$$

where $P_R(\lambda)$ and $P_I(\lambda)$ are obtained from

$$P(\lambda + i) = P_R(\lambda) + i \ P_I(\lambda) \tag{42}$$

by separating real from imaginary terms. To apply this rule we write Eq. (35) as

$$M_{N+1} \ P_M(\lambda + i) = y'_{N+1} \ P_\alpha \ (\lambda + i) + \Theta P_\Theta \ (\lambda + i) \tag{43}$$

Using the definitions of Eq. (37) the multiblade equations are

$$\begin{bmatrix} P_{MR}(\lambda) & P_{MI}(\lambda) \\ - P_{MI}(\lambda) & P_{MR}(\lambda) \end{bmatrix} \begin{bmatrix} M_I \\ M_{II} \end{bmatrix} = \begin{bmatrix} P_{\alpha R}(\lambda) & P_{\alpha I}(\lambda) \\ - P_{\alpha I}(\lambda) & P_{\alpha R}(\lambda) \end{bmatrix} \begin{bmatrix} \alpha_I \\ \alpha_{II} \end{bmatrix}$$

$$- \begin{bmatrix} P_{\Theta I}(\lambda) & - P_{\Theta R}(\lambda) \\ P_{\Theta R}(\lambda) & P_{\Theta I}(\lambda) \end{bmatrix} \begin{bmatrix} \Theta_I \\ \Theta_{II} \end{bmatrix} \tag{44}$$

In the absence of cyclic pitch inputs from the control system we have according to Fig. 10

$$\Theta_I = \lambda_I \quad , \quad \Theta_{II} = \lambda_{II} \tag{45}$$

Inserting Eq. (45) into Eq. (44) one obtains the rotor impedance
matrix in roll and pitch by premultiplying Eq. (44) with

$$
\begin{bmatrix}
P_{MR}(\lambda) & P_{MI}(\lambda) \\
- P_{MI}(\lambda) & P_{MR}(\lambda)
\end{bmatrix}^{-1}
\tag{46}
$$

This completes step 3 of the impedance analysis.

Coupled Rotor/Support Analysis

A coupled rotor/support analysis is performed for the system shown
in Fig. 11. The rotorshaft is assumed to be rigid and connected to a
rigid housing that is supported by an up-focusing mount with focus on
the rotor center. Thus the hub is rigidly restrained against hori-
zontal and vertical motions. The elastic restraints in pitch and roll
are indicated by the horizontal springs attached to the shaft housing.
There also is a gravitational restraint (pendulum effect) that is to
be included in the support stiffness and in the support natural fre-
quency.

The unit for the moments M_I, M_{II} is $\rho_o R^3 \Omega^2$. With the time unit
$1/\Omega$ one then obtains the rotor pitching and rolling moments

$$
(b/2) \; \rho_o \; R^3 \; M_I \quad , \quad (b/2) \; \rho_o \; R^3 \; M_{II}
\tag{47}
$$

For uniform blades

$$
\rho_o \; R^3 = 3 \; I_b
\tag{48}
$$

The rotor support dynamic equations without support damping are

$$
\begin{bmatrix}
\omega_I^2 - \lambda^2 & 0 \\
0 & \omega_{II}^2 - \lambda^2
\end{bmatrix}
\begin{bmatrix}
\alpha_I \\
\alpha_{II}
\end{bmatrix}
= 3(b/2) \; (I_B/I)
\begin{bmatrix}
M_I \\
M_{II}
\end{bmatrix}
\tag{49}
$$

By inserting $\begin{bmatrix} M_I \\ M_{II} \end{bmatrix}$ from Eq. (49) into Eq. (44) one obtains with Eq. (45) a set of homogeneous equations for α_I , α_{II} that are of the form

$$\begin{bmatrix} Q_{11} & Q_{12} \\ Q_{21} & Q_{22} \end{bmatrix} \begin{bmatrix} \alpha_I \\ \alpha_{II} \end{bmatrix} = 0 \tag{50}$$

The coupled system characteristic equation is then given by

$$\begin{vmatrix} Q_{11} & Q_{12} \\ Q_{21} & Q_{22} \end{vmatrix} = 0 \tag{51}$$

The mode shapes are computed by inserting into Eq. (50) one of the eigenvalues obtained from Eq. (51). One then finds that all modes are either regressing or progressing in the rotating reference system. This completes step 4 of the analysis as far as coupled system natural modes and frequencies are concerned. The ratio of the rotor moment on the flexible support over that on a rigid support will be determined from Eq. (17) as a function of the support uncoupled natural frequency. All that is required for this purpose is the knowledge of the uncoupled support frequency $\overline{\omega}_{SN}$ for which the excitation frequency coincides with the coupled system natural frequency.

Computational Limitations

The computations were performed on the IBM-360/65 computer using double precision (16 digits). Single blade computations were made for 5, 8, 10 15 and 20 elements per blade. The number of 20 elements was found to be too high for the 16 digit precision used. With 10 blade elements no computational difficulties were encountered, provided that the evaluation of the 3 by 3 determinant in Eq. (35) was numerically optimized by writing

$$|\ldots| = \phi_{33}(\phi_{24}\phi_{45} - \phi_{44}\phi_{25}) + \phi_{34}(\phi_{23}\phi_{45} - \phi_{43}\phi_{25}) - \phi_{35}(\phi_{23}\phi_{44} - \phi_{43}\phi_{24})$$

(52)

whereby the set ϕ_{33}, ϕ_{34}, ϕ_{35} represents the column with the highest values of the elements. A convenient check for adequate computer precision consists of looking at the coefficients of λ^{nmax}, λ^{nmax+1}, etc., in P_Θ, whereby nmax is the highest power that should occur theoretically in this polynomial. With N point masses nmax = 2N-2 for P_Θ. If the computer precision is adequate, the coefficients of λ^{nmax+1}, λ^{nmax+2}, etc., are several orders smaller than those of λ^{nmax}. The accuracy of the computation depends on how the determinant is evaluated, the method of Eq. (52) giving the best results.

Once the single blade problem could be solved without difficulties, the coupled system solutions posed no further obstacles. The computer accuracy depends on the highest eigenvalue considered and does not suffer when the number of eigenvalues is approximately doubled as for the coupled system, as long as the highest eigenvalue remains approximately the same. The results presented here were obtained with 8 masses per blade. As compared to an analysis with 10 elements per blade the first 3 eigenvalues shown here were found to have less than 1% error. The equivalent CPU time to obtain a complete set of eigenvalues for the coupled system was 4 seconds. For 55 cases computed in one run the CPU time was 34 seconds.

The introduction of more blade degrees of freedom - in-plane bending and torsion - and of a much higher order of the airframe impedance polynomials may not lead to computational difficulties, if the highest eigenvalue of the system is not substantially increased. If numerical difficulties do occur, the method of reference 13 would be helpful. According to this method the order of the characteristic equation is reduced by modalizing and truncating the component mobility matrices and by applying a correction term to the truncated expressions. The method has been successfully applied to the problem of Eq. (51). The results will be reported elsewhere.

Coupled Rotor and Support Modes

The two parameters that determine the dynamics of the uniform blade are the non-dimensional blade bending stiffness q and the Lock number γ. The centrifugal tension force T_i occurring in $p = (T_i/q)^{1/2}$ of Eq. (27) can be easily computed for each blade station i. The blade Lock number occurs as factor in the aerodynamic terms c_i and g_i of Eq. (25). Since $q^{-1/2}$ is proportional to the rotor angular speed it can be used as non-dimensional speed parameter. We select for the numerical example $q^{-1/2} = 18$ and $\gamma = 5$. This results in a blade cantilever first natural frequency in vacuum of 1.06, which is a realistic value for a hingeless rotor. For the first 3 cantilever blade bending modes one then obtains the following complex eigenvalues, whereby R and P denote regressing and progressing modes in the rotating system respectively.

<div align="center">

Rotor Alone, $q^{-1/2} = 18$, $\gamma = 5$

Natural Frequency $\zeta \pm i\omega$

</div>

Flap-Bending Mode	Hingeless Rotor ζ	ω	Hinged Rotor ζ	ω
1R	0	0	-.311	.05
1P	-.616	1.96		1.95
2R	-.327	1.57	-.257	1.57
2P	-.193	3.62		3.57
3R	-.240	3.87	-.229	3.80
3P	-.214	5.87		5.80

For comparision purpose the eigenvalues for the hinged rotor have been added, assuming hinges at the rotor center. Since there is no coupling between blades it is sufficient to perform a single blade analysis,

whereby from Eq. (36) $P_\alpha(\lambda) = 0$. This gives the imaginary parts ω_r in the rotating system. Those in the non-rotating system are obtained by $\omega = \omega_r \pm 1$. The imaginary parts of the eigenvalues are almost the same for hinged and hingeless rotor. The interblade coupling for the hingeless rotor affects only the real parts, that is the damping of the modes. While this damping is the same for progressing and regressing modes of the hinged rotor, it differs for the hingeless rotor. The largest difference is for the first progressing mode where the damping of the hingeless rotor is twice that of the hinged rotor.

The hinged rotor does not couple with the support shown in Fig. 11. The coupling of the hingeless rotor is determined by the support natural frequencies ω_I, ω_{II} and by the parameter $3(b/2) I_b/I$ of Eq. (49). We select the blade number $b = 4$ and the ratio of blade moment of inertia over support moment of inertia of $I_b/I = 5$. We further stipulate $\omega_I = \omega_{II} = \omega_S$ which means equal support stiffness in pitch and in roll. When performing the coupled system analysis it turns out that only the two hingeless rotor modes 1P and 2R substantially couple with the support modes, while the higher rotor modes 2P, 3R, 3P are not much affected by the coupling with the support. The coupling of the 1R mode with the support leaves the imaginary part almost at zero but introduces substantial damping, resulting in a almost aperiodic mode.

When varying the support stiffness expressed in ω_S and keeping all other parameters (q, γ, b, I_b/I) constant, one obtains for the coupled 1P modes the ζ and ω values shown in Fig. 12. The uncoupled values are indicated in dash lines. There is a region of instability indicated by a positive real part ζ between an uncoupled support frequency of 1.5 and 3.0. Soft mounting a hingeless rotor can thus be dangerous. Note that we are not considering so called air resonance where the in-plane regressing mode becomes unstable but that we have here a hingeless rotor progressing flap mode instability on its soft support, that is usually called whirl flutter. Similar results would be obtained for a hinged rotor with sufficiently large off-set of the hinges from the rotor center.

The ζ and ω values of the coupled 2R mode are shown in Fig. 13. This graph is quite similar to Fig. 12 for the 1P mode, except that

there is no unstable region of support stiffness. The damping ratio of the coupled support modes, whether positive or negative, approximately given by ζ/ω, is not large. This justifies the neglect of damping in the next section.

Hingeless Rotor Moment Excitation

In order to find out the effect of rotor and support coupling on the moment transferred from the rotor to the support, we apply Eq. (17) to the pitching and rolling moment.

$$M/M_o = [1 - ((\omega_{SN}/\omega)^2 - 1)/((\omega_S/\omega)^2 - 1)]^{-1} \qquad (53)$$

For a 4 bladed rotor the excitation frequency is $\omega = 4$. For both the 1P mode (Fig. 12) and the 2R mode (Fig. 13) the uncoupled support natural frequency ω_{SN} for which the excitation is in resonance with the coupled rotor-support natural frequency is

$$\omega_{SN} = 3.8 \qquad (54)$$

Thus from Eq. (53)

$$M/M_o = (1 + .10/((\omega_S/4)^2 - 1))^{-1} \qquad (55)$$

with $$M/M_o = 0 \quad \text{for} \quad \omega_S = 4.0 \qquad (56)$$

$$M/M_o = \infty \quad \text{for} \quad \omega_S = 3.8 \qquad (57)$$

The relation of $|M/M_o|$ vs. ω_S is shown in Fig. 14. Note the very steep descent of the curve between $\omega_S = 3.8$ and $\omega_S = 4.0$. Same as for the example of vertical vibrations shown in Fig. 6, the value $|M/M_o| = 1$ is reached asymptotically for large values of ω_S representing high support stiffness. Zero moment transfer from the rotor to the support

is obtained for $\omega_S = 4.0$ when the uncoupled support natural frequency is in resonance with the excitation frequency. If damping had been considered, $|M/M_o|$ would not have reached a value of zero at $\omega_S = 4$ but rather a minimum value different from zero.

The spring moment transferred to the base is according to Eq. (18)

$$M_S/M_o = \overline{\omega}_S^2 / (\overline{\omega}_S^2 - \overline{\omega}_{SN}^2) \qquad (58)$$

This ratio is plotted in Fig. 15 vs. ω_S and shows that it is less than one for $\omega_S < 2.7$ where the system is unstable (Fig. 12). Using DAVI's the base moment could be made almost zero for an uncoupled support frequency of $\omega_S < 3.8$. This condition could be unstable.

Conclusion

1. The method of rotor induced vibration prediction by applying the rotor dynamic forces and moments acting on a rigid support to the flexible airframe can lead to large errors of either over or under prediction of vibrations. This method also cannot account for possible dynamic instabilities from rotor-support coupling.

2. The rotor dynamic forces and moments acting on a rigid support must be corrected by a term that has as a factor the rotor impedance taken at the rotor/airframe interface.

3. A practical way of determining the hingeless rotor impedance matrix for the pitching and rolling moments has been developed by first performing a finite element single blade analysis including aerodynamic terms and by then applying a simple transformation to multiblade impedances.

4. Extensions of the rotor impedance analysis are desirable with respect to the following items:

    4.1 From zero to moderate advance ratio by using constant coefficient multiblade equations.

    4.2 From moderate to large advance ratio where periodic coefficients in multiblade equations are necessary.

4.3 From a 2 by 2 impedance matrix for roll and pitch to a
    higher order impedance matrix to include linear hub forces
    and deflections.

4.4 From rigid to flexible blades in chordwise bending and
    torsion, using the transfer matrices developed in reference
    14 and extending them to include aerodynamics.

4.5 From a simple rotor support to a complete airframe.

References

1. Schrage, D.P. and Peskar, R.E., "Helicopter Vibration Requirements",
   33rd Annual Nat. Forum, Amer. Helicopter Soc., Washington, D.C.,
   May 1977, Preprint No. 77.33-33.

2. MIL-STD-1427B, "Human Engineering Design Criteria for Military
   Systems, Equipment and Facilities", December 1974.

3. Yeates, J.E. Jr., "A Discussion of Helicopter Vibration Studies
   Including Flight Tests and Analysis Methods Used to Determine the
   Coupled Response of a Tandem Type", Journal Amer. Helicopter Soc.
   Vol. 1, No. 3, July 1956.

4. Anderson, W.D. and Gaidelis, J.A., "Vibration Inputs and Response
   of a Hingeless Rotor Compound Helicopter", Lockheed LR 26523,
   June 1974.

5. Staley, J.A. and Sciarra, J.J., "Coupled Rotor/Airframe Vibration
   Prediction Methods", Rotorcraft Dynamics, NASA SP-352, 1974.

6. Gessow, A. and Myers, G.C. Jr., "Aerodynamics of the Helicopter",
   Macmillan Co. 1952.

7. Bramwell, A.R.S., "Helicopter Dynamics", John Wiley, N.Y. 1976.

8. Rita, A.D., McGarvey, J.H. and Jones, R., "Helicopter Rotor
   Isolation Evaluation Utilizing the DAVI", 32nd Annual Nat. Forum,
   Amer. Helicopter Soc., Washington, D.C., May 1976, Preprint
   No. 1030.

9. DesJardins, R.A. and Hooper, W.E., "Antiresonant Rotor Isolation
   for Vibration Reduction", 34th Annual Nat. Forum, Amer. Helicopter
   Soc., Washington, D.C., May 1978, Preprint 78-24.

10. Hohenemser, K. and Yin, S.K., "Some Applications of the Method of Multiblade Coordinates", Journal Amer. Helicopter Soc., Vol. 17, No. 3, July 1972.

11. Isakson, G. and Eisley, J.G., "Natural Frequencies in Bending of Twisted Rotating and Nonrotating Blades", NASA TN D-371, March 1960.

12. Hohenemser, K. and Yin, S.K., "Finite Element Stability Analysis for Coupled Rotor and Support Systems", Part III of Final Report under Contract NAS2-7613, June 1977.

13. Kung, Weih-chi and Hohenemser, K., "Eigenvalue Analysis for Coupled Large Damped Structures", Computer Methods in Applied Mechanics and Engineering, Vol. 12, pp. 69-75, 1977.

14. Isakson, G. and Eisley, J.G., "Natural Frequencies in Coupled Bending and Torsion of Twisted Rotating and Nonrotating Blades", NASA CR-65, July 1964.

List of Figures

Fig.1

Fig.2

Fig. 3

$$\omega_R^2 = K_R/m_R$$

$$f, f_o, z$$

$$\omega_S^2 = K_S/m_S$$
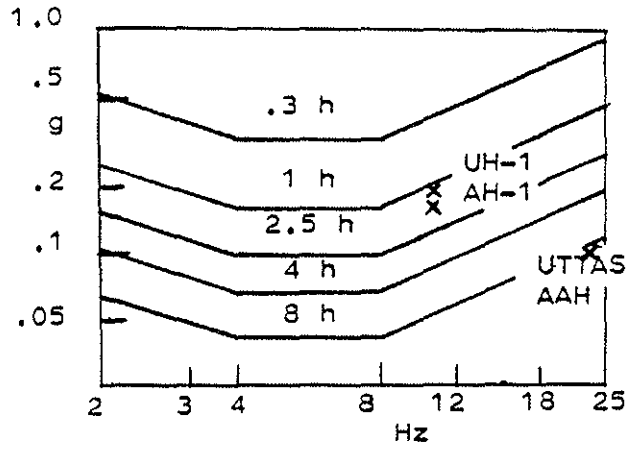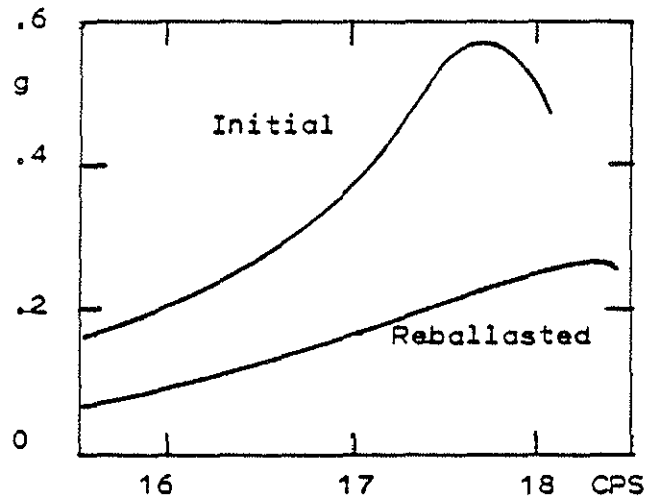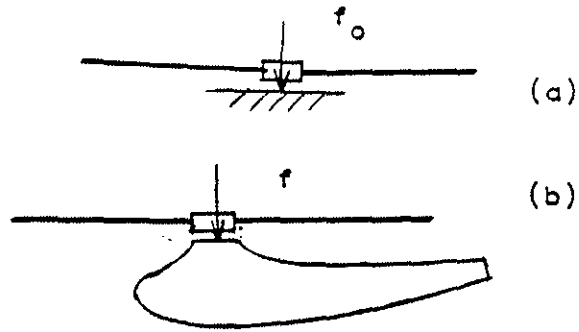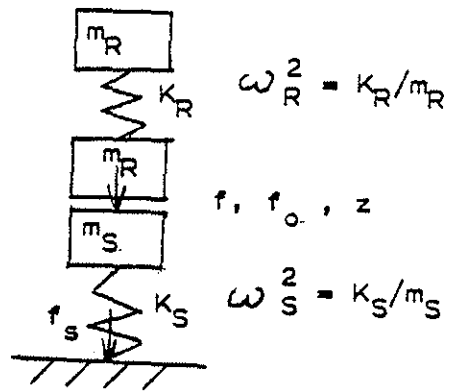
Fig. 4

Fig.5

Fig.6

Fig.7

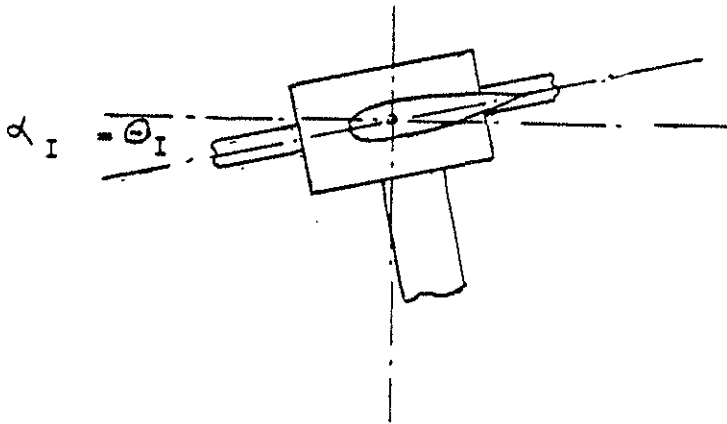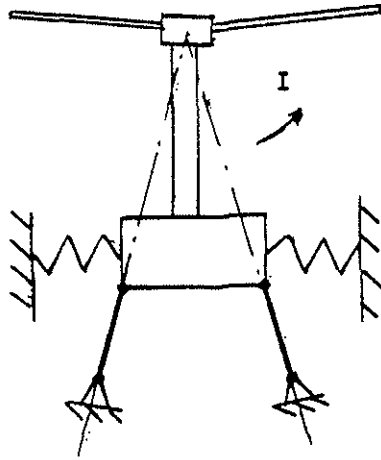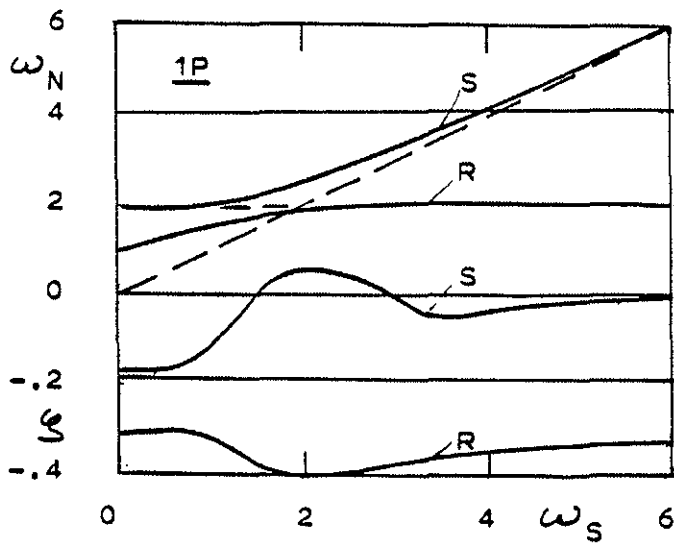$$m_A = m(1/a)^2$$

Fig.8

$$-y_i(\lambda^2 m_i + \lambda c_i) + \theta g_i$$
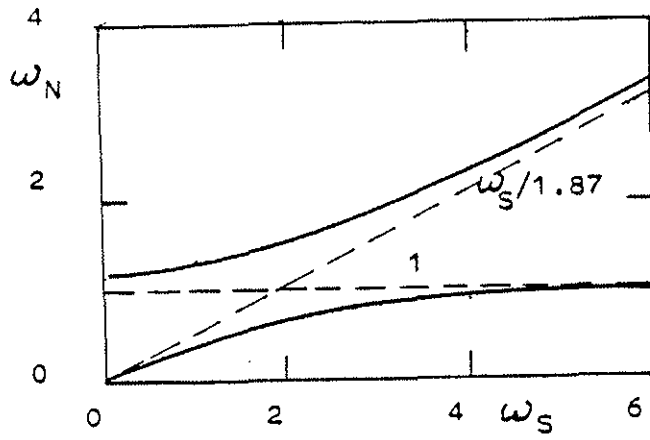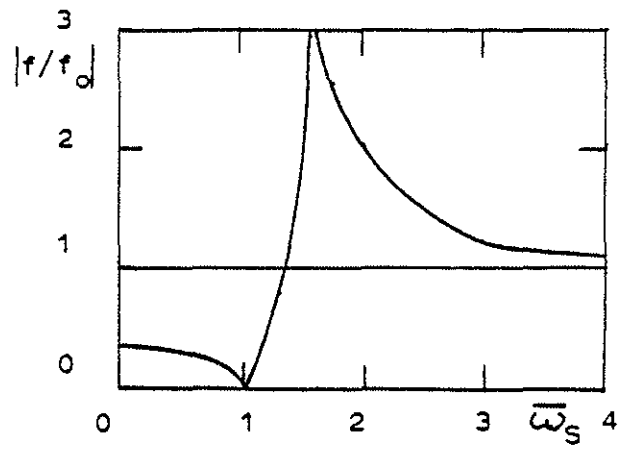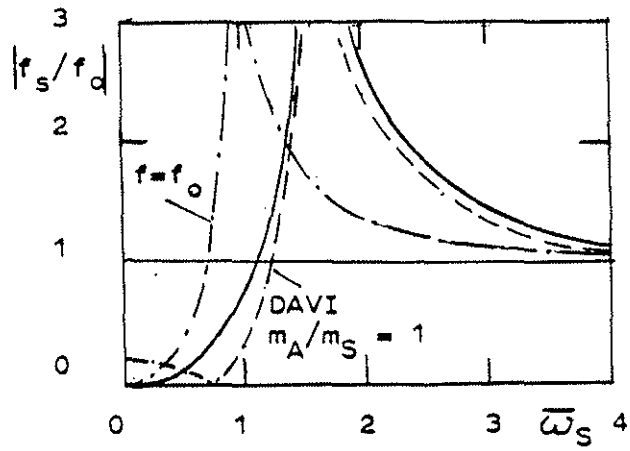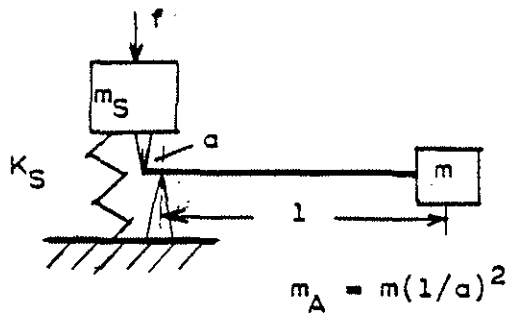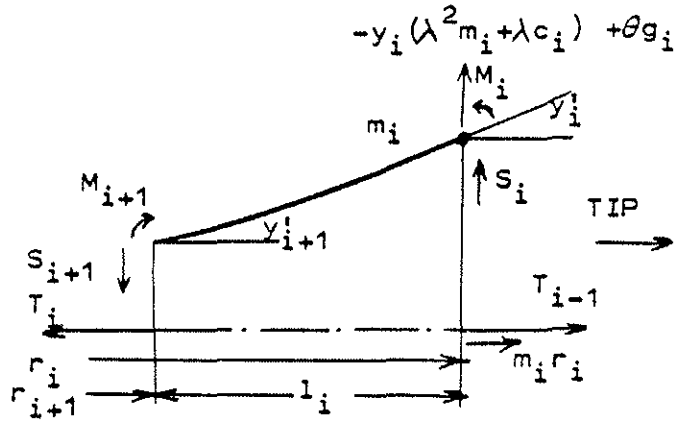
Fig.9

Fig.10

Fig.11

Fig.12

Fig.13

Fig.14

Fig.15

17-34